Geologie en Mijnbouw **73:** 215–223, 1994.

Source parameters of the 1992 Roermond earthquake, the Netherlands, and some of its aftershocks recorded at the stations of the Geological Survey of Northrhine-Westphalia

Rolf Pelzing
Geologisches Landesamt Nordrhein-Westfalen, De-Greiff-Str. 195, 47803 Krefeld, Germany

Received 15 June 1993; accepted in revised form 11 October 1993

Key words: acceleration, fault-plane solution, hypocenter, seismic moment and dislocation, triggered earthquakes

Abstract

The Roermond earthquake of April 13, 1992, was recorded unclipped at four of the six stations of the Geological Survey of Northrhine-Westphalia (epicentral distances between 54 and 103 km). The local magnitude values determined from these recordings are 5.9 for stations GSH, PLH and OLF, and 6.1 for station WBS. The main shock hypocenter was located at latitude 51° 10.1′ N and longitude 5° 55.9′ E at a depth of 17.6 km. The focal mechanism determined from P and SH-wave polarities and amplitude ratios is 120° for strike, 70° for dip, and – 100° for rake, which corresponds to an almost pure dip-slip movement along a normal fault. The mean seismic moment, calculated from several spectra, is 5.4×10^{16} Nm, the mean dislocation is 35 cm. Until the end of May about 80 aftershocks from the Roermond area were recorded at the stations of the Geological Survey. The main shock also triggered a series of earthquakes at the southern border of the Roer Valley Graben between Geilenkirchen and Eschweiler, about 30–45 km SSE of the main shock epicenter. The largest of these events had a local magnitude of $M_L = 3.7$.

Introduction

The Lower Rhine Embayment is one of the main earthquake regions in western Central Europe. Since 30 million years this area is slowly subsiding, causing a fragmentation of the crust into a system of blocks which are tilted to the northeast and separated by deep-reaching active faults (Wrede & Hilden 1988). Some of the main fault systems are those that bound the Roer Valley Graben, an area that moves downward in relation to its surroundings. In some parts of the Roer Valley Graben the Hercynian basement with its Permian-Mesozoic cover is overlain by more than 1000 m of Tertiary and Quaternary. The northeastern boundary is the 'Rurrand' fault in Germany and the 'Peelrand' fault in the Netherlands. This is the place where the Roermond earthquake occurred.

The seismic network of the Geological Survey of Northrhine-Westphalia

In 1980 the Geological Survey of Northrhine-Westphalia (Germany) started operating a local seismic network in the Lower Rhine Embayment and the adjacent parts of the Rhenish Massif. Presently, this network consists of six stations which are shown in Fig. 1. Stations JCK, PLH and GSH were installed in 1980 to 1981, stations KRF and OLF in 1988, and station WBS in 1991 (see Table 2 in Camelbeeck et al. 1994).

Due to the thick cover of Tertiary and Quaternary sediments the seismic noise in the Lower Rhine Embayment is considerably higher than in the Rhenish Massif to the east and south. Therefore, at the stations JCK, PLH, and KRF the seismometers are installed in boreholes which are about 400 m deep and extend down to the consolidated rock of the Hercynian basement. The seismic noise at the bottom of the boreholes is about one tenth of that at the surface and thus com-

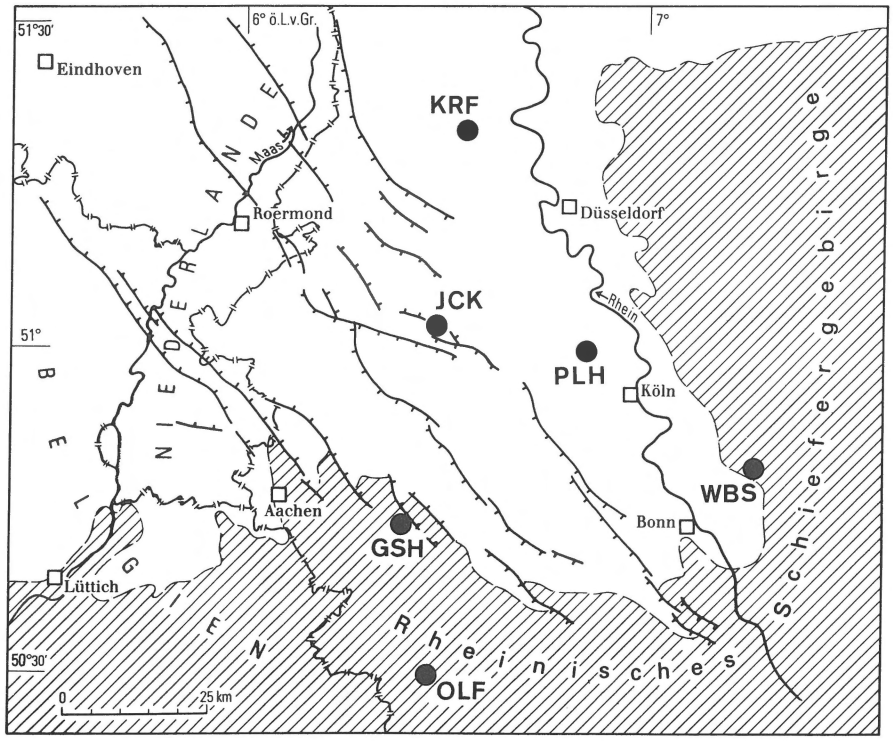

Fig. 1. The six seismic stations of the Geological Survey of Northrhine-Westphalia (•). Stations KRF, JCK, and PLH are borehole stations. The dashed line indicates the outline of the Rhenish Massif. Active faults are shown with barbs on the downthrown side.

parable to the noise conditions at favourable sites in the Rhenis Massif.

All stations are equipped with three-component short period seismometers and digital recording systems. The data are recorded in trigger mode on tape using pulse code modulation (PCM) or on PC hard disk as 16 bit words. Technical details have already been described elsewhere (Pelzing 1990). Stations JCK and GSH are connected to the Geological Survey in Krefeld via telephone lines enabling data transmission on call. Station GSH is also a small tripartite micro-array with a seismometer spacing of about 200 m.

Recordings of the Roermond earthquake

The Roermond earthquake was recorded unclipped at four of the six stations of the Geological Survey of Northrhine-Westphalia. JCK was out of operation due to maintenance work, and the recording at KRF is heavily clipped. The nearest unclipped recordings were obtained from stations GSH (epicentral distance 54 km) and PLH (63 km). The seismograms of these stations are shown in Figs 2 and 3. The local magnitudes (M_L), calculated according to the formula given by Ahorner (1983), are 5.9 for stations GSH, PLH, and OLF, and 6.1 for station WBS.

Since this earthquake is also of considerable interest for engineering applications, the acceleration time history at station GSH is shown in Fig. 4. It is derived from the velocity record by numerical differentiation and thus corresponds to the seismogram shown in Fig. 2. The maximum acceleration in a single component (NS) is 270 mm/s^2. A response spectrum for the two horizontal components was calculated by evaluating the maximum amplitude of single-degree of freedom oscillators with different natural periods and 5% damping, subjected to the acceleration time history as input. The equation of motion was numerically integrated for each oscillator using the Runge-Kutta-Nyström method. The spectrum is shown in Fig. 5, the maximum response is about 1 m/s^2 in the NS component.

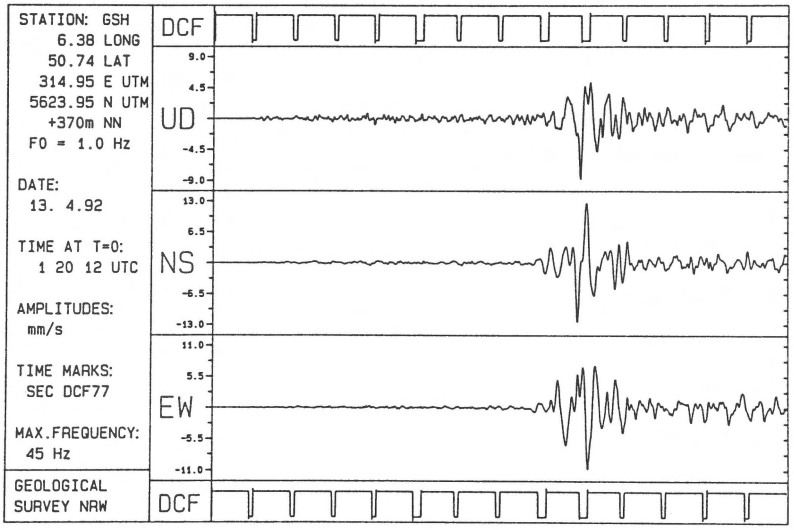

Fig. 2. Seismogram of the Roermond earthquake at station GSH (epicentral distance 54 km). UD is the vertical, NS the north-south, and EW the east-west component. DCF indicates the time signal of the long-wave DCF 77 transmitter. The pulses are one second apart.

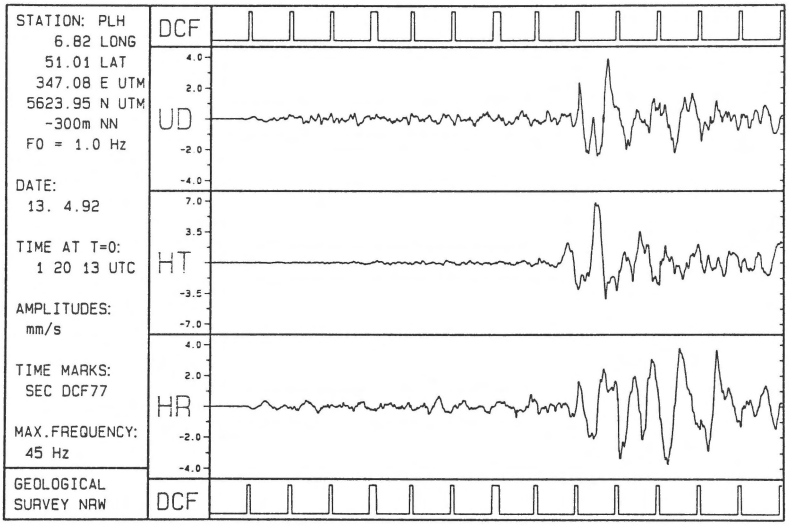

Fig. 3. Seismogram of the Roermond earthquake at station PLH (epicentral distance 63 km). UD is the vertical, HT the horizontal tangential, and HR the horizontal radial component. DCF as in Fig. 2.

Location of the main shock

The precise location of the main shock hypocenter is complicated by the fact that no seismic station existed in the epicentral area at the time of the earthquake. Therefore, depth determination is very sensitive to slight changes of the velocity model. Most of the stations operating at that time are to the east and especially to the south of the epicenter.

The model used for location is shown in Fig. 6. It is a simplification of a model derived by Ahorner (Ahorner & Pelzing 1985). The P-wave velocity in the upper part down the Moho is given by the formula $v(z) = 5.0 + (6.15 - 5.0) \times (z/15)^{1/2}$, where z is depth, and 5.0 and 6.15 are the P-wave velocities at 0 and 15 km depth, respectively. The P- and S-wave velocity ratio is assumed to be 1.7. The location method is the usual Geiger method. Travel times for the velocity model are calculated numerically by a grid method

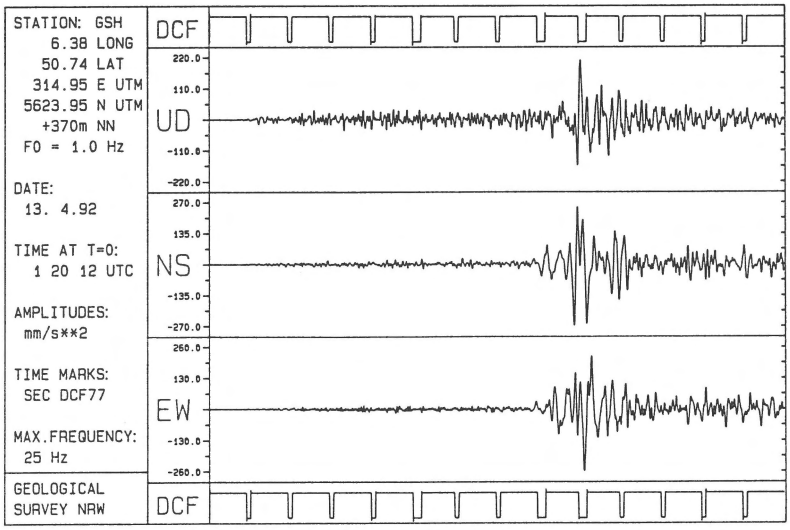

Fig. 4. Accelerogram at station GSH. The unit is mm/s^2. The components and the time section are the same as in Fig. 2.

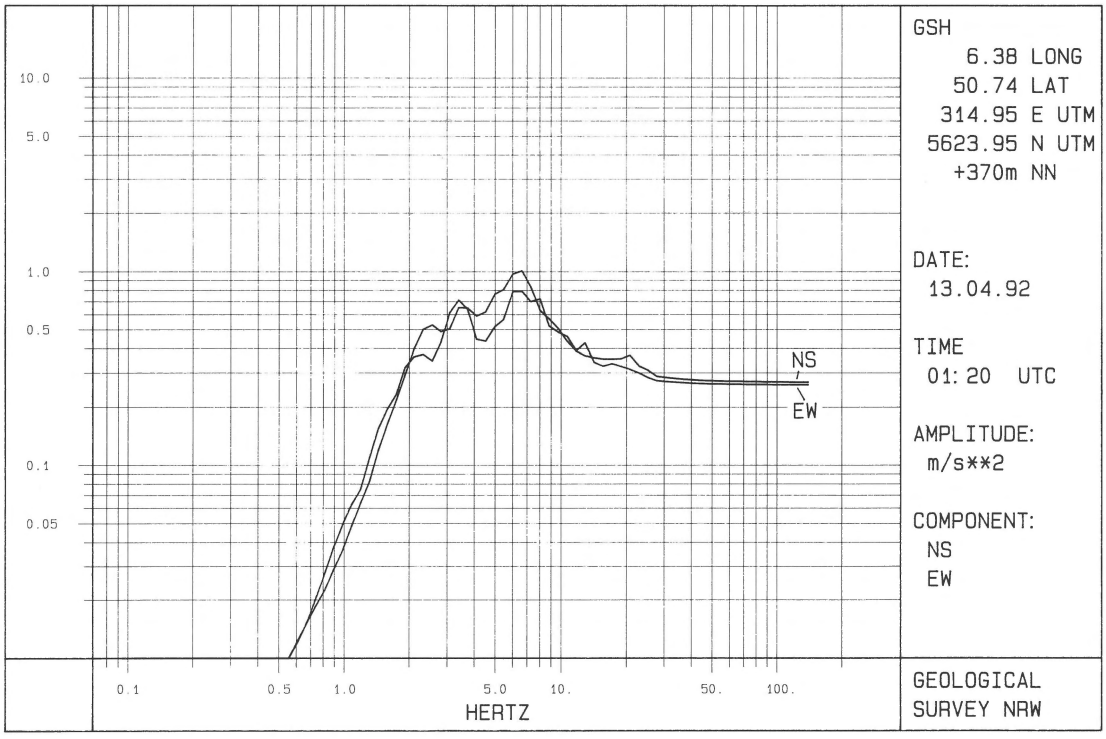

Fig. 5. Response spectra for the two horizontal components at station GSH, derived from the accelerograms in Fig. 4. The amplitude unit is m/s^2. The maximum response is about 1 m/s^2 in the NS component.

Table 1. Source parameters for the main shock obtained from P and S-wave spectra of individual stations. Corner frequency (fc), source radius (R), source area (F), logarithm of seismic moment ($\log(M_0)$), stress drop (SD), and dislocation (D). P and S-wave sprectra interpretations are based on the source model of Brune (Lee & Stewart 1981: 159)

Station	Wave type	fc (Hz)	R (km)	F (km^2)	$\log(M_0)$ (N*m)	SD (MPa)	D (cm)
PLH	P	1.6	1.4	6.5	16.60	5.8	20
WBS	P	1.4	1.7	8.6	16.85	6.9	27
PLH	S	1.0	1.4	5.8	16.58	6.6	21
GSH	S	1.2	1.1	4.0	16.82	19.9	54
OLF	S	1.1	1.2	4.8	16.82	15.3	46
WBS	S	1.2	1.1	4.0	16.73	16.2	44
Mean values:			1.3	5.6	16.73	11.8	35

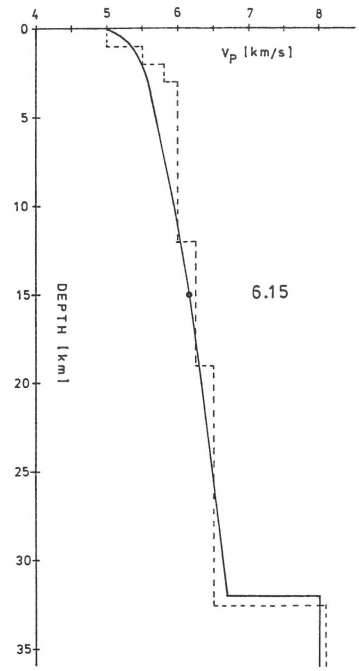

Fig. 6. P-wave velocity-model used for the location of main shock and aftershock hypocenters (solid line). Its upper part is a parabola $v(z) = 5 + (6.15 - 5) \times (z/15)^{1/2}$, where z is depth, and 5 and 6.15 are the velocities at 0 and 15 km depth, respectively. The parabola ends at the Moho of 32 km depth. The dashed line is a model derived by Ahorner for the Lower Rhine Embayment (Ahorner & Pelzing 1985).

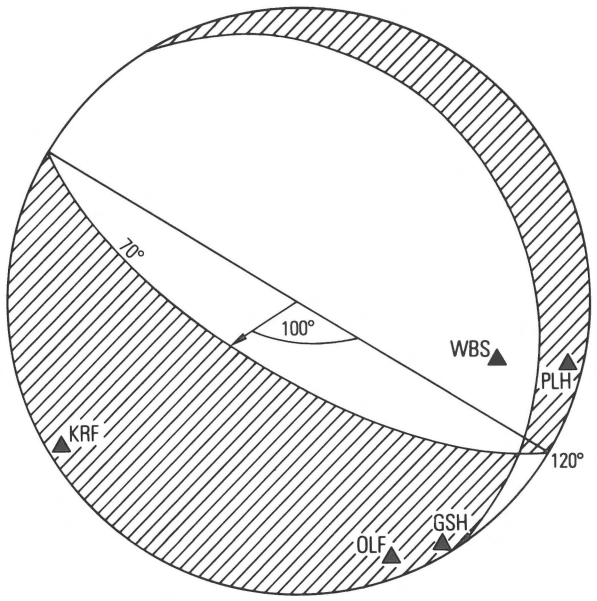

Fig. 7. Fault-plane solution for the Roermond earthquake (lower hemisphere projection). P-wave first motion compression is observed in the hatched areas, dilatation in the blank areas. Strike is 120°, dip is 70°, and rake is – 100°. The accuracy is estimated to ± 10° for each angle. The three-letter codes refer to stations indicated in Fig. 1.

(Pelzing 1978). By using the arrival times of 15 stations in Belgium, the Netherlands, and Germany at epicentral distances up to about 100 km the following coordinates for the main shock hypocenter were calculated:

latitude	51° 10.1′ N
longitude	5° 55.9′ E
depth	17.6 km
origin time	01:20:02.4 UTC

The precision is estimated to be 1 to 2 km for the epicentral coordinates and 3 to 4 km for depth.

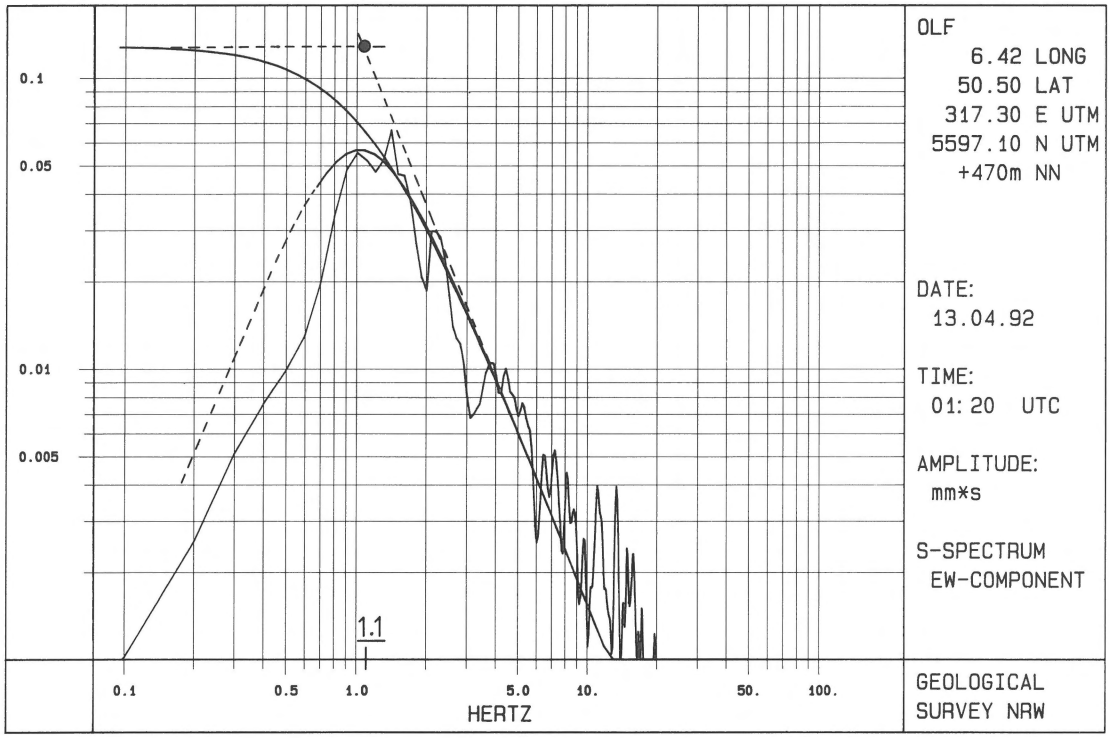

Fig. 8. S-wave spectrum (EW component) at station OLF (epicentral distance 84 km) and corresponding omega-square-model curves. The partly dashed curve indicates the best-fit theoretical curve for 0.7 to 10 Hz containing the instrumental response (natural period 1 Hz, damping 62%). The uppermost curve is the corresponding model curve without instrumental response and has a corner frequency of 1.1 Hz.

Source parameters of the main shock

The focal mechanism was determined from P and SH-wave polarities and amplitudes from the recordings of the Geological Survey. First, these recordings were rotated horizontally into radial and transverse components with respect to the direction to the epicenter. Then P and SH-wave amplitudes were determined (including signs) and corrected for surface effects. The fault plane solution was obtained by a grid search procedure with a 5° spacing for strike, dip and rake. In a first step all grid points were discarded which did not give the correct P-wave polarities. For the remaining points the observed P and SH amplitudes were combined to a vector and normalized to one. The same was done for the theoretical amplitudes as given by Aki & Richards (1980: 115). The largest sum of inner products between observed and calculated vectors for all stations was chosen as the best fit solution and resulted in 120° for strike, 70° for dip, and – 100° for rake, following the nomenclature of Aki & Richards (1980: 106). The precision is estimated at about ± 10° for each angle. The focal mechanism solution, which corresponds to an almost pure dip-slip, is shown in Fig. 7 and is in good agreement with well-constrained solutions based on a large number of P-wave polarities, as given by, for example, Ahorner (1992).

Several P and S-wave spectra were calculated from the unclipped recordings and corrected for absorption with a Quality factor Q of 500. Theoretical frequency curves for the omega-square-model (Aki & Richards 1980: 823), multiplied by the seismometer response, were fitted to the spectra between 0.7 and 10 Hz. The corner frequencies were then obtained by correcting the best-fit model curves for the seismometer response. An example is shown in Fig. 8. From the corner frequencies and the corresponding low-frequency levels numerical values for seismic moment, source radius, stress drop, and dislocation were calculated based on the model of Brune (Lee & Stewart 1980: 159). The mean values are 5.4×10^{16} Nm for seismic moment and 35 cm for dislocation. Data and results are listed in Table 1.

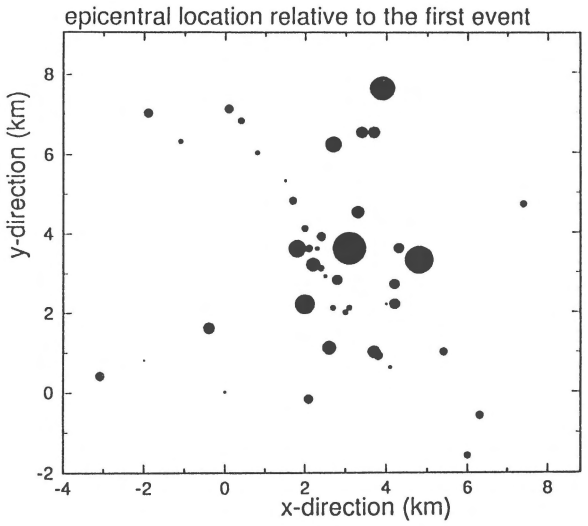

Fig. 9. Map showing the relative location of epicenters of the cluster of events between April 13 and May 31, 1992 in the Eschweiler-Alsdorf area, about 30–45 km SSE of the main shock epicenter. The diameter of the dots is proportional to magnitude; the largest event has magnitude $M_L = 2.8$. Positive y corresponds to North and positive x to East direction.

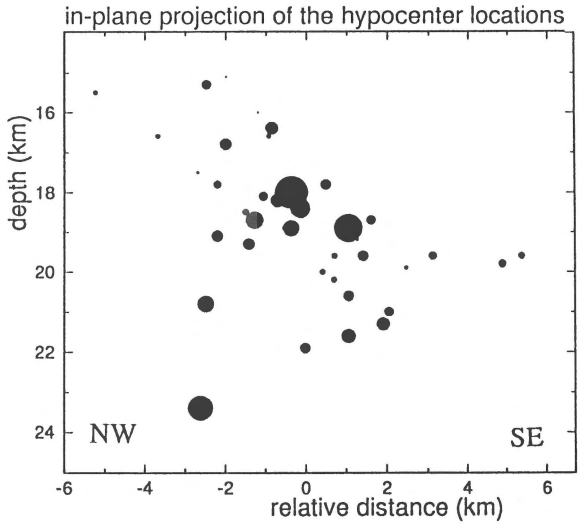

Fig. 10. NW (left)-SE (right) section through the crust showing the depth distribution of the events in Fig. 9. Hypocenters are projected on a vertical NW-SE plane.

Table 2. Parameters of three earthquakes in Northrhine-Westphalia triggered by the Roermond main shock. The favoured focal mechanism is solution I in all cases

Date	April 13	April 14	April 14
Time UTC	04:32:47.4	01:06:46.0	01:36:23.2
Local magnitude	2.4	3.7	2.8
Longitude E	6° 15.5′	6° 10.7′	6° 14.1′
Latitude N	50° 50.2′	50° 58.0′	50° 49.9′
Focal depth (km)	18.9	9.8	18.0
Strike I	130°	95°	140°
Dip I	60°	80°	40°
Rake I	− 50°	− 125°	− 50°
Strike II	250°	350°	290°
Dip II	50°	40°	50°
Rake II	− 140°	− 20°	− 110°

Aftershocks

The Roermond earthquake was followed by a considerable number of aftershocks in the source region (Camelbeeck et al. 1994). It also triggered a series of smaller earthquakes at the southern border of the Roer Valley Graben in Germany, most of which form a cluster between the towns of Eschweiler and Alsdorf, about 30–45 km SSE of the main shock epicenter. The seismic activity in this area began about 40 minutes after the main shock and had its maximum with respect to both magnitude and number of events in the evening of April 13 and the early morning of April 14.

The main cluster of events between Eschweiler and Alsdorf occurred in an area that displays more or less continuous microseismic activity since the installation of stations nearby. Figure 9 shows the epicenters of the located events between April 13 and the end of May 1992. Figure 10 is a NW-SE section through the crust showing the depth distribution of these same events. The Feldbiß and Sandgewand faults are the main faults bordering the Roer Valley Graben to the southwest, but there are other parallel faults in that area as well. As their continuation with depth is not very well known, the hypocenters cannot be assigned with certainty to a specific fault. It is also possible that more than one fault was active.

Three events of the 'southern group' were more closely examined (Table 2, Fig. 2). The first, an M_L = 2.4 earthquake at 04:32 UTC on April 13, was the largest of these events during the first few hours after the main shock. The second is an $M_L = 3.7$ earthquake southeast of Geilenkirchen at 01:06 UTC on April 14. Its seismogram at station GSH is shown in Fig. 11. This was the largest event triggered by the Roermond main shock, and was also strongly felt. Its epicenter is somewhat to the north of the main cluster of events

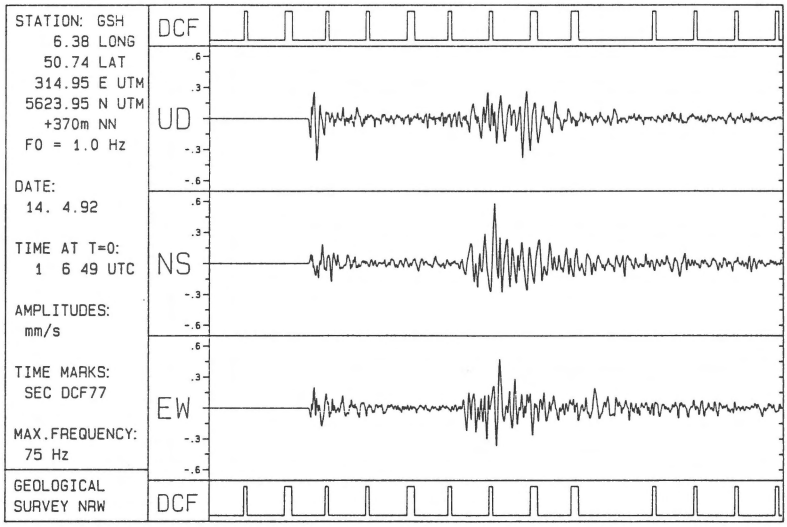

Fig. 11. Seismogram of the largest event triggered by the Roermond main shock at station GSH (April 14, 0.1:06 UTC, $M_L = 3.7$). Components and time marks as in Fig. 2.

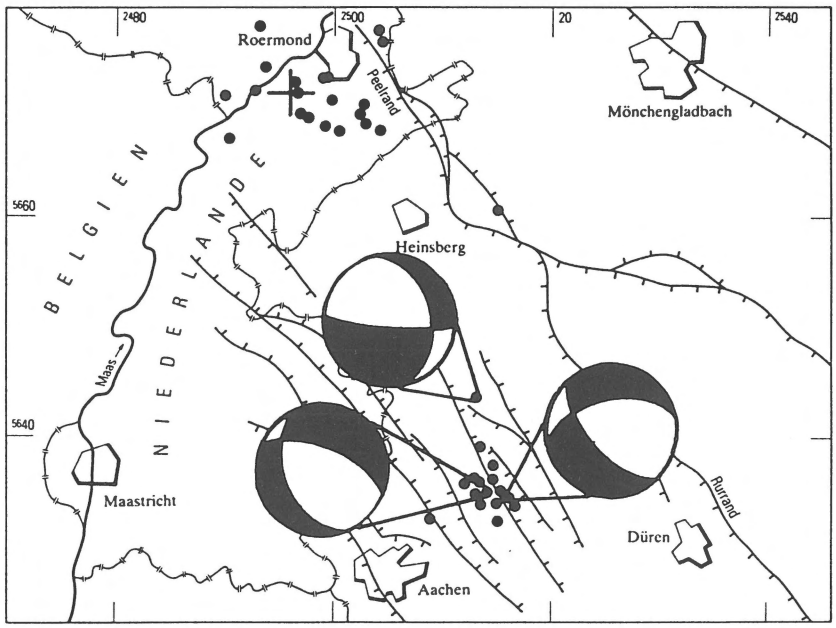

Fig. 12. Lower hemisphere projections of the fault-plane solutions for three earthquakes triggered by the Roermond main shock, about 30–45 km SSE of the main shock epicenter (cross). The upper one is April 14, 01:06 UTC, the left one April 13, 04:32 UTC, and the right one April 14, 01:36 UTC. In the focal-plane solutions, black quadrants indicate P- wave first motion compression, blank quadrants dilatation. Dots indicate epicenters of some of the aftershocks and triggered events. Coordinates according to Gauss-Krueger system.

between Eschweiler and Alsdorf. The third event is an $M_L = 2.8$ earthquake at 01:36 UTC on April 14, which is the largest in the main cluster itself.

For the three last-mentioned events fault-plane solutions were obtained using the same method as for the main shock (Fig. 12). The two events of 04:32 UTC on April 13 and 01:36 UTC on April 14 have fault planes in accordance with the main strike direction of many active faults in that area. The favoured mechanism is an oblique-slip mechanism, at which the southwestern fault side has moved downward and southeastward in relation to the northeastern side. The

mechanism of the event on April 14, 01:06 UTC is not so clearly correlated to the strike of known faults. It is probably a downward and westward movement of the southern side of the fault relative to the northern side. Focal angles and hypocentral coordinates of the three events are given in Table 2.

In total, about 160 events were recorded at the stations of the Geological Survey of Northrhine-Westphalia until the end of May 1992. Approximately half of this number originated from the Roermond area, the other half from the southern border of the Roer Valley Graben. Since then the seismic activity in the Lower Rhine Embayment has returned to its previous level, with occasional events still occurring in both areas.

References

Ahorner, L. 1983 Historical seismicity and present-day microearthquake activity of the Rhenish Massif, Central Europe. In: K. Fuchs, K. von Gehlen et al. (eds): Plateau Uplift – Springer, Berlin: 198–221

Ahorner, L. 1992 Das Erdbeben bei Roermond am 13. April 1992 – Bericht der Abteilung für Erdbebengeologie des Geologischen Instituts der Universität zu Köln. Bensberg, 11 pp

Ahorner, L. & R. Pelzing 1985 The source characteristics of the Liège earthquake on November 8, 1983 from digital recordings in West Germany. In: P. Melchior (ed.): Seismic Activity in Western Europe – D. Reidel Publ. Co., Dordrecht: 263–289

Aki, K. & P.G. Richards 1980 Quantitative Seismology – W.H. Freeman and Co., San Francisco, 932 pp

Camelbeeck, T., T. van Eck, R. Pelzing, L. Ahorner, J. Loohuis, H.W. Haak, P. Hoang-Trong & D. Hollnack 1994 The 1992 Roermond earthquake, the Netherlands, and its aftershocks – Geol. Mijnbouw, this issue

Lee, W.H.K. & S.W. Stewart 1981 Principles and Applications of Microearthquake Networks – Academic Press, New York, 293 pp

Pelzing, R. 1978 Untersuchungen zur Ortung von Herden seismischer Ereignisse, dargestellt an Beispielen aus einem Stationsnetz im Ruhrbergbaugebiet – Ber. Inst. Geophys. Ruhr-Univ. Bochum 6: 184 pp

Pelzing, R. 1990 The seismic network of the Geological Survey of North Rhine-Westphalia and the seismic activity of the Lower Rhine area from 1980 to 1988 – Cah. Centre Europ. Géodyn. Séismol. 1: 75–84

Wrede, V. & H.D. Hilden 1988 Geologische Entwicklung. In: Geologie am Niederrhein – Geologisches Landesamt Nordrhein-Westfalen, Krefeld: 7–14